Available online at www.sciencedirect.com

ScienceDirect

Physica E 40 (2008) 1851–1854

PHYSICA E

www.elsevier.com/locate/physe

Phase-coherent transport in a mesoscopic few-layer graphite wire

T. Ihn*, D. Graf, F. Molitor, C. Stampfer, K. Ensslin

Solid State Physics Laboratory, ETH Zurich, 8093 Zurich, Switzerland

Available online 15 September 2007

Abstract

Four-terminal magnetotransport measurements have been performed on a mesoscopic graphite wire with a thickness of about seven graphene layers in which the carrier density can be tuned via the field effect using a back gate and in-plane gates. The conductance measured as a function of back gate voltage and temperature can be well described by the simple two-band model. Measurements of Shubnikov–de Haas oscillations agree well with the parameters extracted at zero magnetic field with the help of the model. Measurements of the weak localization correction to the conductivity and conductance fluctuations confirm the mesoscopic character of electronic transport and allow to estimate the phase-coherence length to be of the order of the wire length (several microns) at the lowest temperatures. The results are compatible with electron–electron interactions being responsible for decoherence at the lowest temperatures.

© 2007 Elsevier B.V. All rights reserved.

PACS: 73.20.Fz; 73.23.−b; 73.40.−c

Keywords: Mesoscopic transport; Weak localization; Universal conductance fluctuations; Graphene

Thin monocrystalline graphitic films have recently proven to be of fundamental scientific interest and are predicted to have a great potential for future applications in electronics [1]. We have studied mesoscopic electronic transport in a few-layer graphene wire at low temperatures. While the elastic mean free path is small compared to the dimensions of the wire, the phase coherence length exceeds its width and is comparable to its length at the lowest temperatures.

Our sample shown in Fig. 1(a) was prepared by mechanical exfoliation and deposition on a standard Si/SiO_2 substrate which led to a wire of $W = 320\,\mathrm{nm}$ width. The height of the flake was 3.2 nm corresponding to about seven stacked graphene layers. Cr(5 nm)/Au (90 nm) contacts and side gates (widths and gaps 0.5 μm) were evaporated onto and next to the wire. The length between the two inner ohmic voltage contacts was $L = 2.5\,\mu\mathrm{m}$, the contact resistance was of the order of 1 kΩ. The four metallic side gates and a back gate allowed to alter the conductance via the field effect [2]. Four terminal measurements were performed by applying an AC signal of 100 nArms to the outer contacts (o_L, o_R) and measuring the voltage drop between the inner contacts (i_L, i_R) at temperatures between 1.7 and 100 K.

The filled circles in Fig. 1(b) show the measured resistance as a function of back gate voltage V_{bg} at the temperature $T = 1.7\,\mathrm{K}$. The behavior of the resistance as a function of V_{bg} and temperature can be described with the simple two band model [3], where the bandstructure of graphite is represented by overlapping parabolic valence band ($E = E_0/2 - \hbar^2k^2/2m^*$) and conduction band ($E = -E_0/2 + \hbar^2k^2/2m^*$) dispersions. The three-dimensional density of states for valence and conduction band is taken to be $4m^*/\pi\hbar^2 c_0$, where c_0 is twice the interlayer separation. Within this model we use an effective lever arm $\alpha = 1/(1 + d/(\varepsilon\lambda_s)(1 - e^{-d_{gr}/\lambda_s}))$, where d is the thickness of the silicon oxide and d_{gr} that of the graphitic wire [5]. The gate potential is assumed to be screened exponentially in the z-direction of the flake according to $\Phi(z, V_{bg}) = \alpha(V_{bg} + V_0)\,e^{-z/\lambda_s}$ as shown in Fig. 1(c) for different back gate voltages. For the sheet electron and hole densities we write $n_{e/h}(E_F, T) = (4m^*/\hbar^2\pi c_0)(k_B T \cdot \log(1 + e^{(E_0/2 \pm E_F)/k_B T}))$. By fitting the measured resistance curve in Fig. 1(b) we find an energy overlap $E_0 = 2.8\,\mathrm{meV}$ and an effective electron mass of $m_e^* = 0.041 m_e$, which agrees well with previously reported data on thin graphite flakes [2,4,5].

*Corresponding author. Tel.: +41 1 6332280; fax: +41 1 6331146.
E-mail address: ihn@phys.ethz.ch (T. Ihn).

1386-9477/$ - see front matter © 2007 Elsevier B.V. All rights reserved.
doi:10.1016/j.physe.2007.08.092

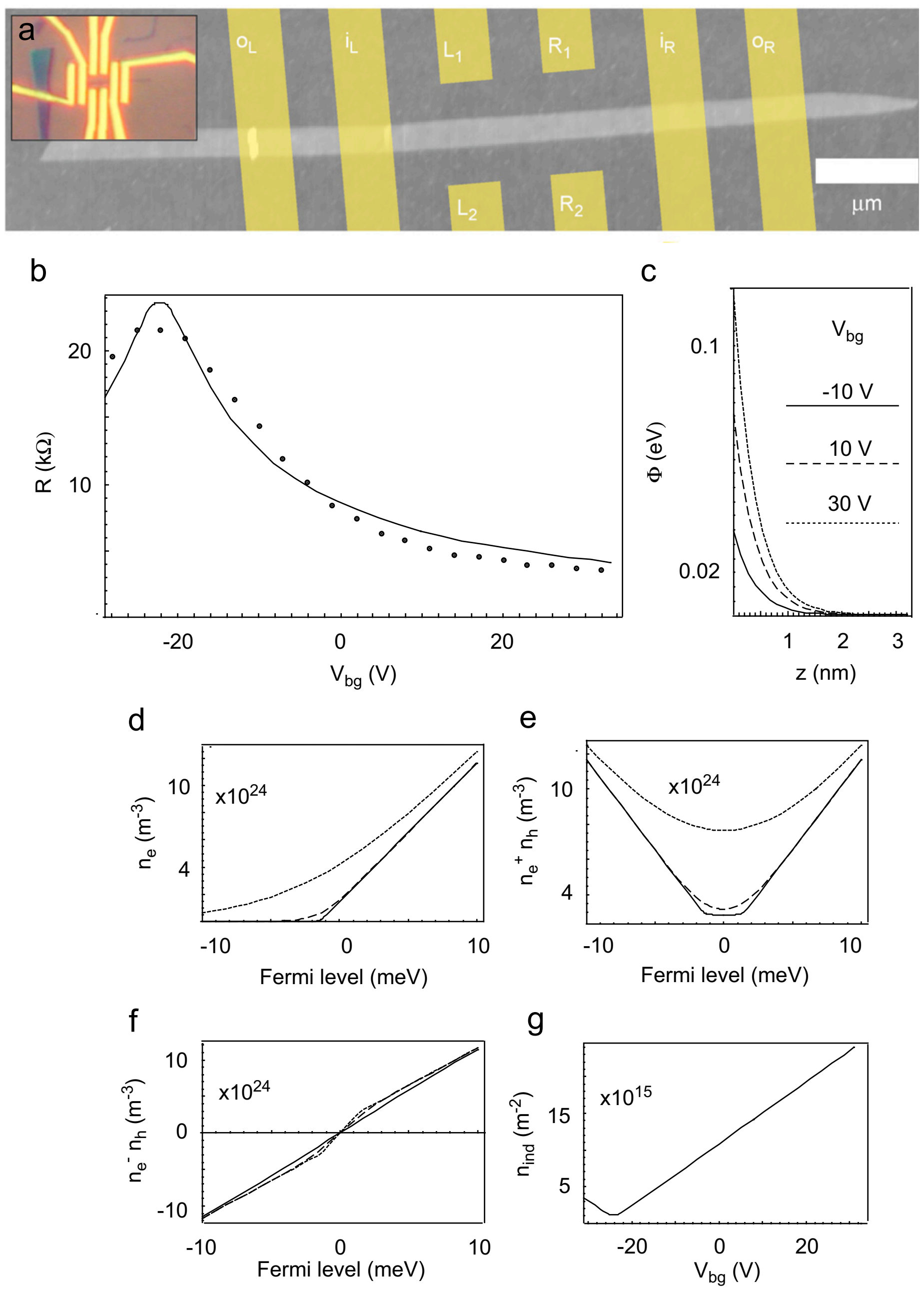

Fig. 1. (a) SFM micrograph of the graphite wire with a schematic of the four contacts (i_L, i_R, o_L, o_R) and four side gates (L_1, L_2, R_1, R_2). (b) Simple two band model fit (solid line) to the resistance data (dots) measured at $T = 1.7$ K. (c) Electrostatic potential (or change in Fermi energy) induced by the back gate in the graphitic flake along the c-axis for three different voltages ($V_{bg} = -10$, 10 and 30 V). The interface is at $z = 0$ nm. (d) Total (bulk) electron density n_e, (e) combined total (bulk) electron and hole densities ($n_e + n_h$) and (f) difference between total (bulk) electron and hole densities as a function of Fermi level with the parameter extracted from the fit in (b) for three different temperatures (solid: $T = 1.7$ K, dashed: $T = 10$ K and dotted: $T = 50$ K). The resistance maximum is set to $E_F = 0$ meV. (g) Induced 2D carrier density as a function of back gate voltage at $T = 1.7$ K calculated with the parameter taken from the fit in (b) including the shift of the resistance maximum.

At finite temperature, near the resistance maximum the Fermi–Dirac distribution populates electron and hole states at the band edges leading to an enhanced total carrier density and thus to a reduced sample resistance [$R = L/W(n_e + n_p)e\mu$]. The calculated total bulk electron density is shown in Fig. 1(d), and the combined total bulk electron and hole densities in Fig. 1(e) as a function of Fermi level for three different temperatures ($T = 1.7$, 10 and 50 K). 'Total bulk' refers here to the integration (from $z = 0$ to 3.2 nm) along the z-direction. For completeness also the difference ($n_e - n_h$) is presented in Fig. 1(f). For large back gate voltages far away from the mixed region in the regime of pure electron transport thermal smearing of the Fermi edge will not change the overall density as long as $k_B T \ll E_F$. The electron mobility estimated from this model in the regime of pure electron transport yields about

2700 cm^2/Vs at $T = 1.7$ K. Therefore, the mean free path $l_e \approx 70$ nm is smaller than the wire width [2].

The measured magnetoresistance of the sample for various back gate voltages is shown in Fig. 2(a)–(e). At high magnetic fields the resistance curves show clear Shubnikov–de Haas minima at magnetic field values that depend on the applied back gate voltage. The minima in the resistance occur when the filling factor $\nu = nh/eB$ is integer. For a fixed filling factor we can write $V_{bg} \propto n = g\nu eB/h$ where g accounts for the degeneracy in addition to the spin degeneracy. In Fig. 2(f) we plot the position of the minima in the B–V_{bg} plane together with the linear fits. The latter cross the vertical axis at $V_{bg} = -24.15$ V in agreement with the zero field resistance curve in Fig. 1(a). We identify the filling factors $\nu = 2, 3, 4$ and 5 with $g = 4$ as shown in the inset of Fig. 2(f). The degeneracy accounts for the four atoms in the unit cell of graphite. The degeneracy factor g has been chosen such that the extracted density is equal to the induced 2D density shown in Fig. 1(g) calculated with the fit parameters.

We have extensively studied mesoscopic transport phenomena arising due to quantum interference of charge carriers in the system [6]. In Fig. 3 we show the weak localization correction of the conductance as a function of magnetic field at different gate voltages (a) and for different temperatures up to 30 K (b). A detailed analysis of the data in terms of the theory for one-dimensional systems in the dirty metal regime [6] allows us to extract the

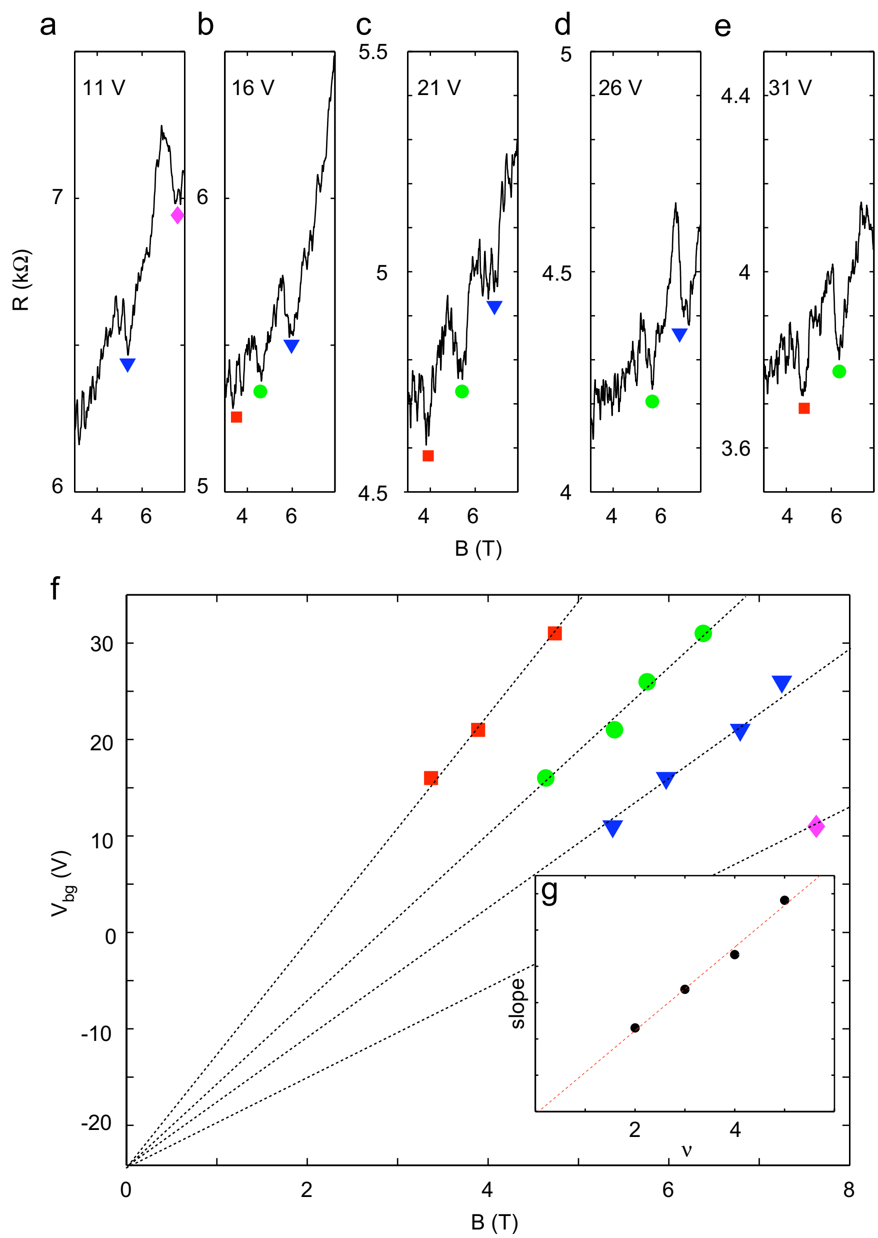

Fig. 2. Resistance as a function of magnetic field for $V_{bg} = 11$ V (a), 16 V (b), 21 V (c), 26 V (d) and 31 V (e). Marked minima are related to Shubnikov–de Haas oscillations. (f) Minima in (a)–(e) parameterized in magnetic field (horizontal axis) and back gate voltage (vertical axis). Inset: Slopes (dots) extracted from the dotted line in (f) as a function of filling factor ν along with a linear fit (dotted line).

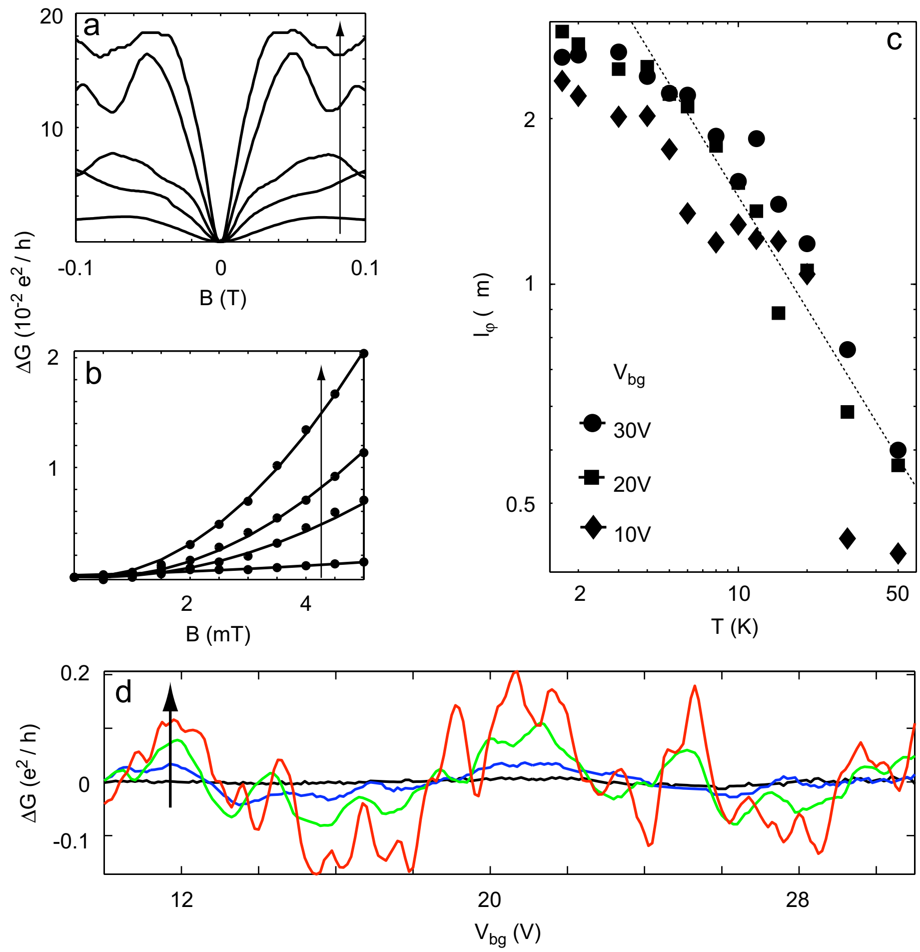

Fig. 3. Weak localization (a) for increasing back gate voltage (direction of the arrow: −10, 0, 10, 20, 30 V) and (b) for increasing temperature (dots, direction of the arrow: 30, 12, 6, 2 K) with corresponding fits using the theory for the dirty metal regime (solid lines). All the curves are normalized to $B = 0$ T. (c) Phase coherence length as a function of temperature for back gate voltages $V_{bg} = 10, 20, 30$ V in a double logarithmic plot. Dotted line represents a power law fit in the range $T \geqslant 4$ K. (d) Conductance fluctuations in back gate voltage for different temperatures (100, 15, 6, 1.7 K) at $B = 0$ T and grounded side gates. A linear background has been subtracted.

phase-coherence length which reaches about three microns at the lowest temperatures and follows a $T^{-0.69}$ power-law dependence as shown in Fig. 3(c). The phase-coherence length turns out to increase linearly with conductivity. This behavior indicates that electron–electron scattering dominates decoherence at the lowest temperatures.

Reproducible quantum conductance fluctuations as a function of back gate voltage are shown in Fig. 3(d) for different temperatures. Similar fluctuations are found as a function of magnetic field [6]. We find that the magnetic field averaged amplitude δG of the fluctuations shows a $G^{1.64}$ power-law dependence on the conductance G. Combining this result with the above finding that the phase coherence length is proportional to G, we obtain the theoretically predicted power law dependence $\delta G \propto l_{\varphi}^{3/2}$, where l_{φ} is the phase-coherence length [6]. At finite magnetic field we find the expected reduction of the conductance fluctuation amplitude by a factor of $2^{-1/2}$ as a result of the breakdown of time-reversal symmetry.

References

[1] A.K. Geim, K.S. Novoselov, Natur. Materials 6 (2007) 183.
[2] K.S. Novoselov, et al., Science 306 (2004) 666.
[3] C.A. Klein, J. Appl. Phys. 35 (1964) 2947.
[4] S. Morozov, et al., Phys. Rev. B 72 (2005) 201401.
[5] Y. Zhang, et al., Phys. Rev. Lett. 94 (2005) 176803.
[6] D. Graf, F. Molitor, T. Ihn, K. Ensslin, Phys. Rev. B 75 (2007) 245429.